Supporting Information for

A Single Molecule Spectroscopic Investigation of Energy Migration Processes in Cyclic Porphyrin Arrays

Mira Park,[†] Min-Chul Yoon,[†] Zin Seok Yoon,[†] Takaaki Hori,[‡] Xiaobin Peng,[‡] Naoki Aratani,[‡] Jun-ichi Hotta,[#] Hiroshi Uji-i,[#] Michel Sliwa,[#] Johan Hofkens,[#,] Atsuhiro Osuka,[‡,*] and Dongho Kim[†,*]*

[†] Center for Ultrafast Optical Characteristics Control and Department of Chemistry, Yonsei University, Seoul 120-749, Korea, [‡]Department of Chemistry, Graduate School of Science, Kyoto University, Sakyo-ku, Kyoto 606-8502, Japan, [#]Department of Chemistry, Katholieke Universiteit Leuven, Celestijnenlaan 200F, 3001 Heverlee, Belgium.

E-mail:dongho@yonsei.ac.kr,osuka@kuchem.kyoto-u.ac.jp, johan.hofkens@chem.kuleuven.be

This PDF file includes:

Figures 1 to 5

References

Supporting Information 1

In a porphyrin monomer, there are two orthogonal transition dipoles B_x and B_y which are degenerate. With an increase in the number of porphyrin units, the low-energy B-band shifts to red, while the high-energy B-band locates nearly at the same position as that of **Z1**, resulting in a progressive increase of the splitting energy in the order **Z2** < **2Z2** < **C12Z**. Therefore, the absorption spectra of **Z2**, **2Z2**, and **C12Z** show electronically allowed two B-bands (S_2 state) and Q-band (S_1 state) with weak absorbance as a result of coupling between vibronic states despite of electronically forbidden state. The absorption spectra of **Z4**, **2Z4**, and **C24Z** are also explained with the same exciton coupling scheme of **Z2**, **2Z2**, and **C12Z**.

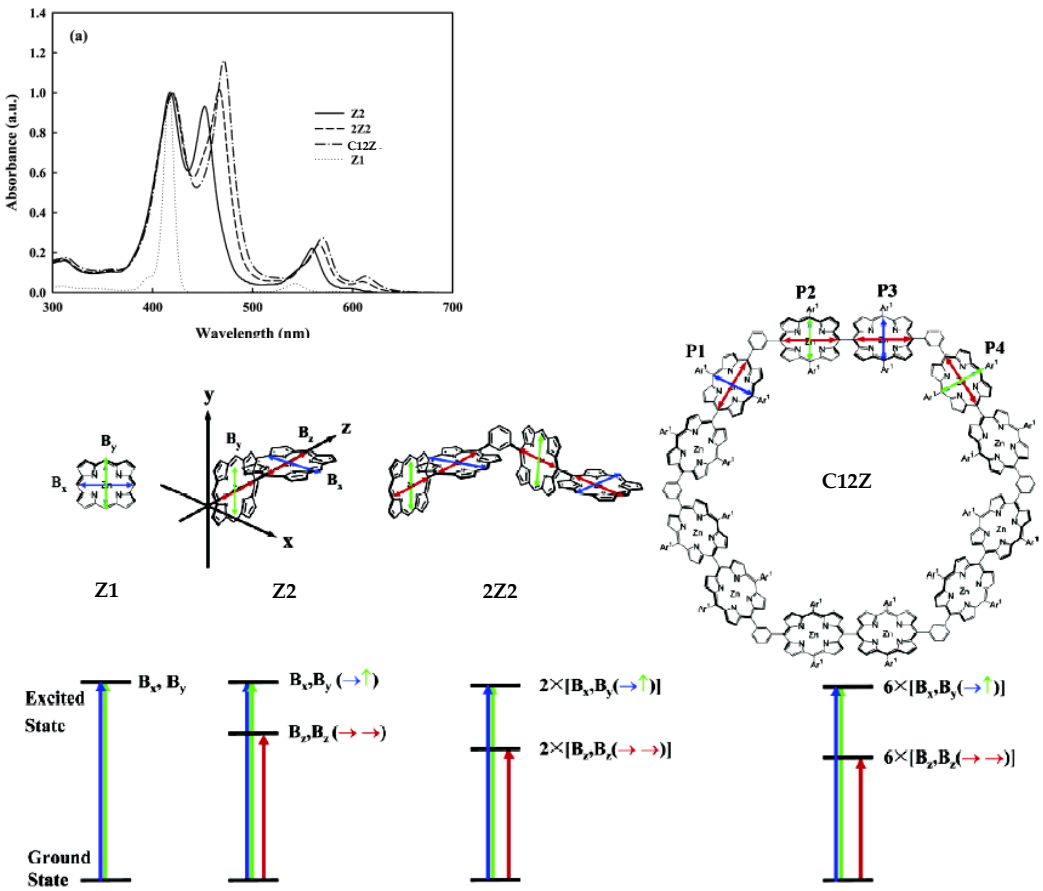

Although we didn't measure the orientation of emission dipoles by the Q-band (568 nm) excitation in the wide-field defocused imaging, we think the optical properties measured at

488 nm will be the same as the result measured by Q-band excitation. The detection of emission dipole orientation by low-energy B-band excitation should be similar to the results by Q-band excitation because the population in the excited S_2 state in porphyrin arrays exhibits a very fast transition (internal conversion) to the S_1 state with less than 100 fs. In addition, the orientation of transition dipole of low-energy B-band is the same as that of the Q-band, along the long molecular axis as shown in above scheme. This was confirmed by the anisotropy fluorescence excitation spectra of directly linked porphyrin arrays, which show a negative anisotropy value at high-energy B-band in contrast with a positive anisotropy value at both low-energy B-band and Q-band

Supporting Information 2

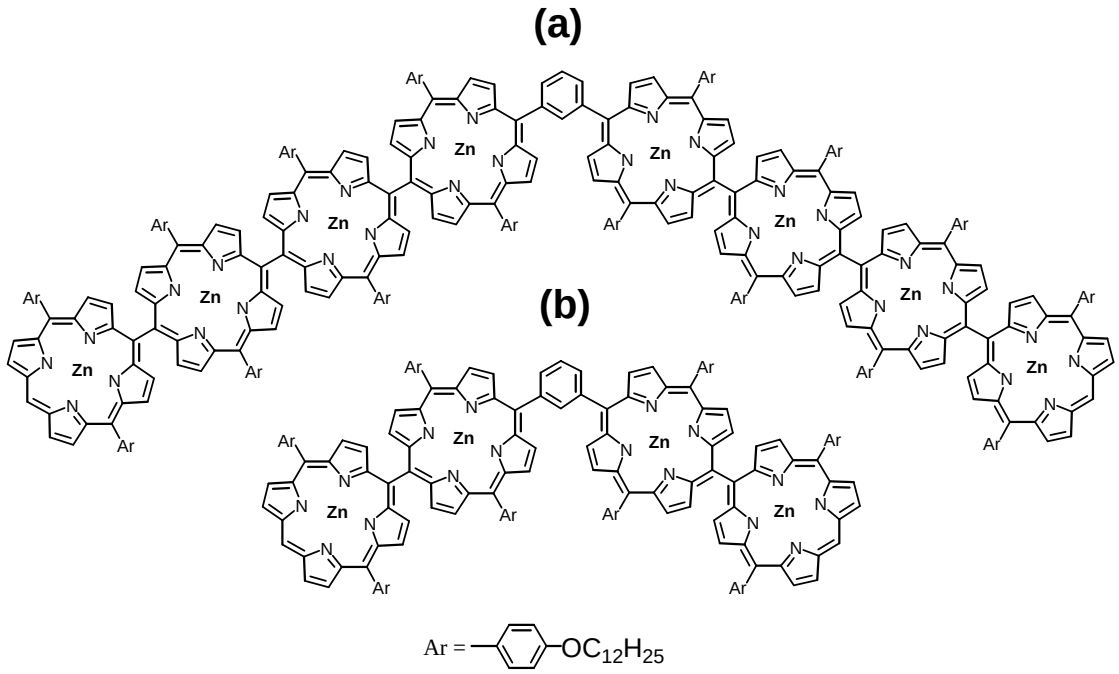

Molecular structures of **2Z4** (energy migration time between tetramer subunits, ~33 ps) (a) and **2Z2** (energy migration time between dimer subunits, ~9 ps) (b). They are respectively composed of two *meso*-*meso* linked tetraporphyrins **Z4** and diporphyrins **Z2** bridged by a 1,3-phenylene linker.

Supporting Information 3

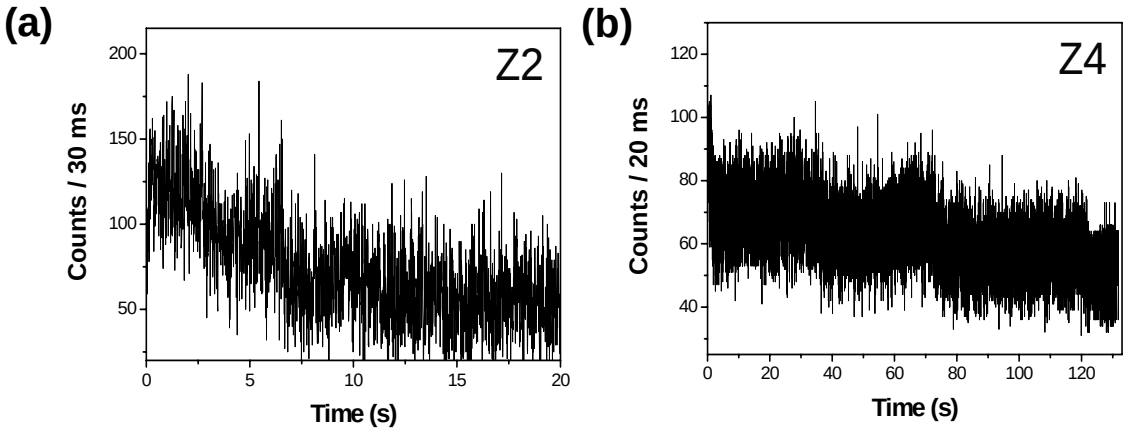

Under atmospheric conditions, the representative fluorescence trajectories of reference linear arrays **Z2** and **Z4** are shown under identical experimental conditions i.e., average excitation power of 1 μW using 543.5 nm continuous wave excitation light. For **Z2**, the subunit of **L12Z** and **C12Z**, and for **Z4**, the subunit of **C24Z**, the fluorescence intensity trajectories exhibit double and quadruple stepwise photobleaching without long off-times, respectively. The details on the setup were documented in a relevant previous paper.[1]

Supporting Information 4

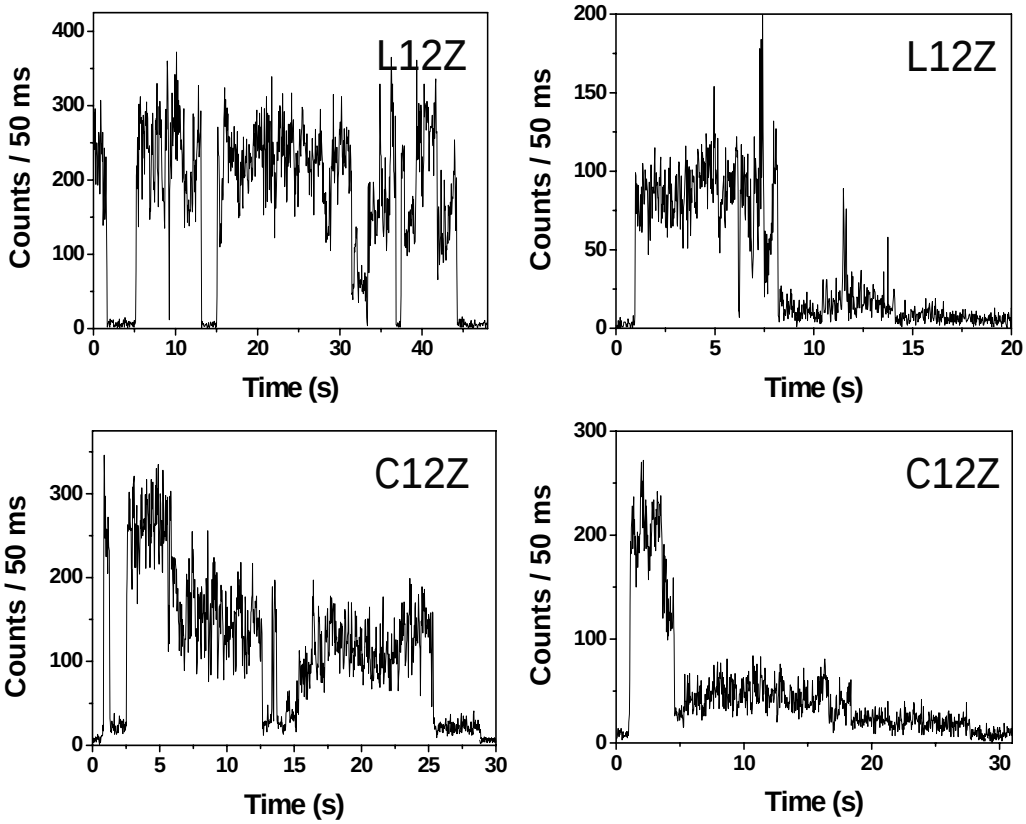

Fluorescence intensity trajectories of 1,3-phenylene-bridged Zn(II) porphyrin linear array, **L12Z** and cyclic array **C12Z** embedded in a PMMA polymer matrix are shown under atmospheric condition. The fluorescence intensity trajectories exhibit stepwise photobleaching with and without off-times of several seconds. In 56% and 27% of investigated fluorescence intensity trajectories in **L12Z** and **C12Z**, respectively, off-times of several seconds were obtained. The frequent occurrence of off-times can be explained in terms of the existence of nonradiative decay channels, in this case probably related to the flexible conformation of **L12Z** that leads to more frequent occurrences of kink structures.

Supporting Information 5

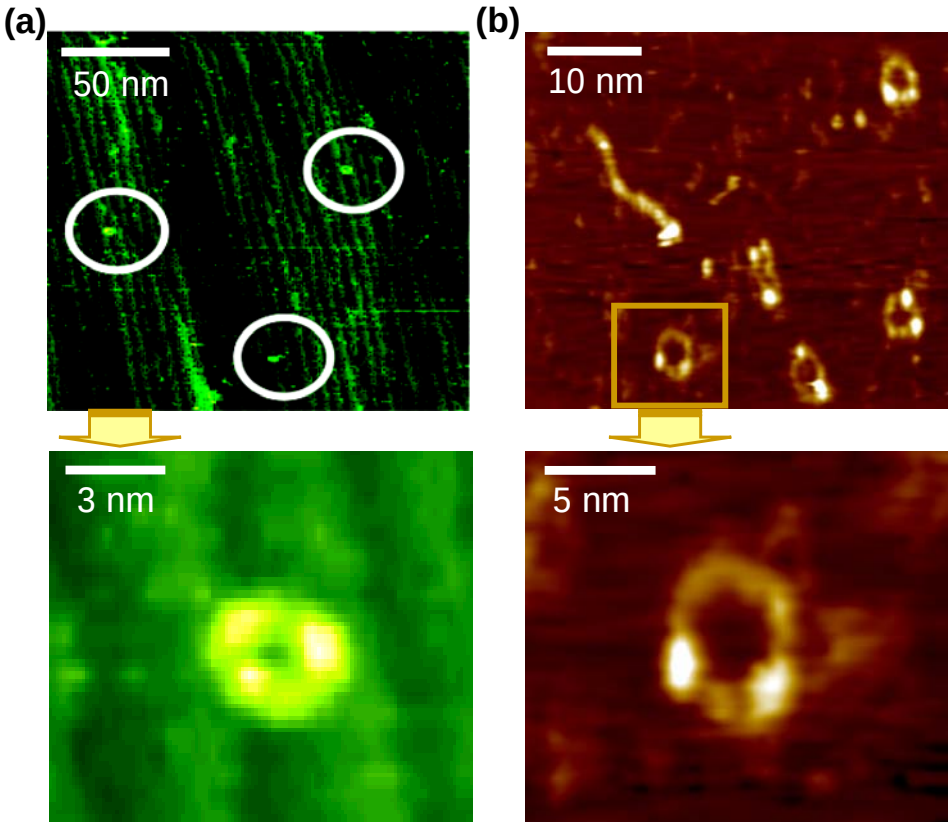

The STM images of **C12Z** (a) and **C24Z** (b) exhibit wheel-like structures. A dilute solution of **C12Z**[2] in CH_2Cl_2 and **C24Z**[3] in CH_2Cl_3 was sprayed by using a pulse injection method onto a clean Cu(100) surface obtained by cycles of annealing (580°C) and Ar^+ sputtering. STM measurements were performed at room temperature under ultra-high vacuum ($<10^{-10}$ mbar) in a constant height or current mode by using an electrochemically etched Pt/Ir tip. The STM images of **C12Z** taken at sample bias voltage (V_s) of 1.5 V and tunneling current (I_t) of 37 pA reveal ring spots with discrete hollow. An average height of the STM images estimated on the basis of the height histogram is ca. 2.9 ± 1.2 Å and an average diameter is 35 ± 6.7 Å, being similar to a calculated diameter of ca. 36-38 Å for **C12Z**. The STM images of **C24Z** taken at sample bias voltage (V_s) of 1.5 V and tunneling current (I_t) of 12.8 pA reveal elliptic rings with hollows. These deformed images of **C24Z** imply conformational flexibility compared with images of uniform **C12Z** (ca. 35 Å diameter). The averaged diameter of the STM images of **C24Z** is 45-70 Å, which matches roughly with its calculated diameter (ca. 70 Å diameter).

References for Supporting Information

1. Park, M.; Cho, S.; Yoon, Z. S.; Aratani, N.; Osuka, A.; Kim, D. *J. Am. Chem. Soc.* **2005**, *127*, 15201.
2. Peng, X.; Aratani, N.; Takagi, A.; Matsumoto, T.; Kawai, T.; Hwang, I.-W.; Ahn, T. K.; Kim, D.; Osuka, A. *J. Am. Chem. Soc.* **2004**, *126*, 4468.
3. Hori, T.; Aratani, N.; Takagi, A.; Matsumoto, T.; Kawai, T.; Yoon, M.-C; Yoon, Z. S.; Cho, S.; Kim, D.; Osuka, A. *Chem. Eur. J.* **2006**, *12*, 1319.